Influence of bromine on the incomplete devil's staircase behavior of betaine calcium chloride dihydrate

Yu. I. Yuzyuk,* A. Almeida, M. R. Chaves, and Filipa Pinto
Departamento de Física, IFIMUP, Faculdade de Ciências da Universidade do Porto, Rua do Campo Alegre, 687, 4169-007 Porto, Portugal

A. Klöpperpieper
Fachbereich Physik, Universität des Saarlandes, 66041, Saarbrücken, Germany
(Received 25 July 2000; revised manuscript received 10 April 2001; published 9 October 2001)

The results of a comparative Raman study of pure and Br^--doped betaine calcium chloride dihydrate in the temperature interval 12–292 K are presented. The analysis of the low-frequency Raman spectra at room temperature revealed that the lowest-frequency phonons are associated with the betaines' vibrations whereas the lattice modes sensitive to Cl^-/Br^- substitution are found above 44 cm^{-1}. The mechanisms responsible for the incommensurate phase are not strongly affected by bromination in contrast with what happens in the commensurate phases. It is shown that bromine weakens hydrogen bonding, preventing the localization of protons related to the onset of the nonmodulated ferroelectric phase. A quantitative analysis of low-frequency spectra provides evidence for a correlation between the anomalous increase of the damping parameter of the activated acoustic mode and the freezing of the random distribution of solitons at low temperatures.

DOI: 10.1103/PhysRevB.64.174106 PACS number(s): 77.80.−e, 64.60.Cn, 63.20.−e, 63.50.+x

I. INTRODUCTION

The fixing of modulation wave vectors and the stabilization of incommensurate (INC) phases are interesting phenomena caused by the presence of imperfections in modulated structures. The microscopic mechanisms leading to these effects are not well understood and more extended experimental studies are needed to clarify the role played by the different defects in the crystal lattice. Betaine calcium chloride dihydrate $(CH_3)_3NCH_2COO\cdot CaCl_2\cdot 2H_2O$ (BCCD) is a remarkable example of a crystal that presents a rich sequence of one-dimensional modulated [$\mathbf{q}=\delta(T)\mathbf{c}^*$] commensurate (C) and INC phases (''incomplete devil's staircase''), occurring between a normal (N) paraelectric and a nonmodulated ferroelectric (FE) phase.[1–10] The temperature ranges of stability of the principal phases at normal pressure are displayed in Table I. The intrinsic properties of BCCD are well known as crystals of high quality can be obtained. Recently, Schaack and Le Maire presented an extensive review of the available experimental information on the modulated phases of BCCD.[11] It is an interesting crystal with delicately balanced intra- and intermolecular interactions, which are very sensitive to external forces or to lattice defects. A small concentration of impurities changes strongly its intrinsic properties, which makes this system particularly attractive for the study of defects in modulated structures. Below $T_i=164$ K the modulation is sinusoidal, whereas on approaching the lock-in (INC-C) transition to the first principal 1/4 C phase, it transforms gradually to a square-wave (solitonic) modulated configuration, where commensurate regions (domains) are separated by solitons (domain walls) or discommensurations. Such a periodic structure is called a ''solitonic lattice.'' The periodicity of solitons can be easily destroyed by defects, such as Br^- impurity, or some other intrinsic pinning centers. Very strong pinning of the modulation can be induced by x-ray irradiation in BCCD: high-order C phases are stabilized and domains of different commensurability coexist in a large temperature interval.[12] Similar effects were observed for small concentrations of bromine (4% and 8%) in BCCD at low temperatures.[13,14]

TABLE I. Domains of stability of the principal phases in BCCD at normal pressure (Refs. 5, 7, and 10).

$\delta(T)=m/n$ (m,n integers)	Temperature range (K)	(Super)space group
Normal	above 164	$Pnma$
INC	128-164	$P(Pnma):1s\bar{1}$
2/7	125-127	
INC	115-125	$P(Pnma):1s\bar{1}$
1/4	76-115	$P2_1ca$
1/5	53-75	$P2_12_12_1$
1/6	47-53	$P2_1ca$
0/1	below 46	$Pn2_1a$

According to x-ray-diffraction (XRD) data[4] in the N phase of BCCD (space group $Pnma$, $Z=4$) the Ca^{2+} ions and the betaine molecules occupy fourfold special positions in the m mirror plane. All the other atoms are localized in eightfold general sites. Two Cl^- ions, two water molecules, and two oxygen atoms of the carboxyl group of the betaines coordinate the Ca^{2+} ions. As shown in Fig. 1 the crystal structure of BCCD is characterized by zigzag chains, forming layers normal to the b direction and lying in the m planes at $y=1/4b$ and $y=3/4b$. O—H$\cdots$Cl bonds between the two inorganic ''Ca'' complexes, lying in neighboring layers, interconnect these layers. The oxygen atoms of the water molecules are coordinated to the Ca^{2+} ions and both the hydro-

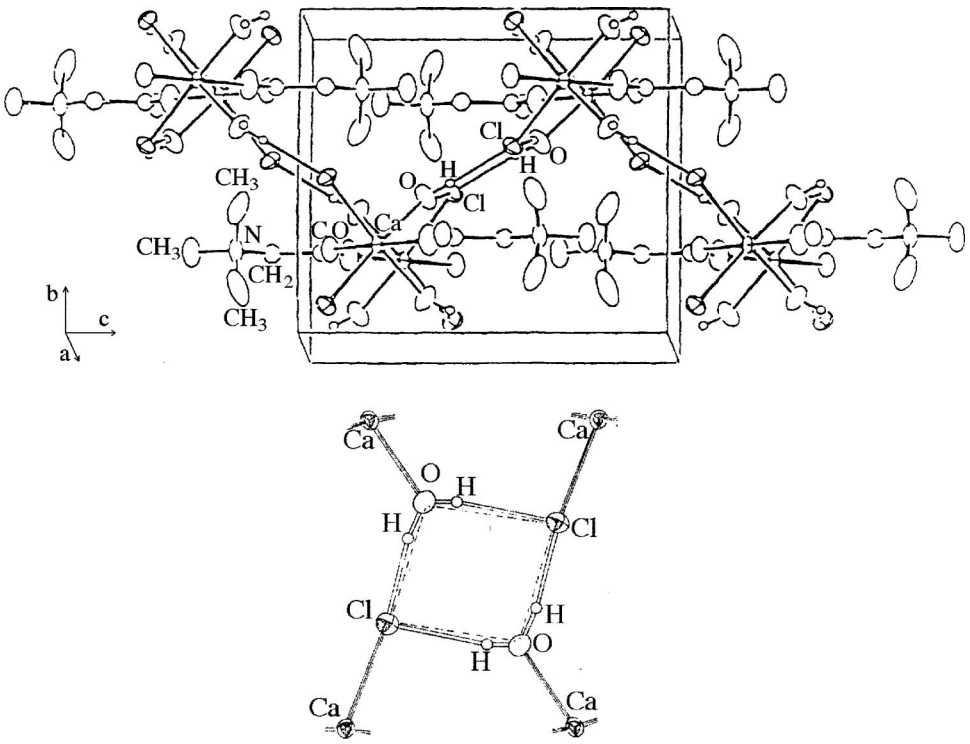

FIG. 1. The unit cell of BCCD in the N phase (Ref. 4). Neighboring layers normal to the *b* direction are connected via hydrogen bonds as shown below.

gens of the water molecules form bonds with Cl^- ions. In fact, the two water molecules and the two Cl^- ions form a slightly distorted parallelogram with unequal O—H$\cdots$Cl bonds along each side. A simple estimation based on the XRD data of Brill *et al.*[4] shows that in the N phase the O—H bond-length difference for the water molecules in the parallelogram is about 9%. Consequently, hydrogen bonds must be very sensitive internal probes of the modulation in BCCD.

The deformation of the crystal structure by the modulation wave is rather complex and available information can be found in Ref. 11 and references therein. It can be approximately represented by a bending of the whole molecule through the connection between the betaine group and the ''Ca'' complex, the bending axis approximately perpendicular to the main axis of the molecule, lying in the *ac* plane. While the betaine molecule can be considered as an almost rigid unit, the 'Ca'-complex is deformed by modulation. The modulation can be visualized roughly as a corrugation of the *ac* layers.[11] In all C phases the unit-cell enlargements occur along the *c* axis.

The partial replacement of Cl^- by Br^- in BCCD leads to a new system (BCCD:Br) displaying rather peculiar properties.[11] For a concentration (x) smaller than 38%, the room-temperature crystal structure of the solid solution is the same as in pure BCCD. As the Br^- ionic radius is larger than that of Cl^- ($r_{Br^-}=0.195$ nm, $r_{Cl^-}=0.181$ nm), a partial bromination breaks the local symmetry and increases the average size of the unit cell (negative chemical pressure). In Br^--doped crystals the phase-transition temperatures shift towards lower temperatures. As long as x increases, the temperature range of stability of the INC phase increases at the expense of the neighboring C phases. These phases are suppressed in samples with $x>15\%$, while the INC phase remains up to $x\approx 30\%$. The dielectric anomalies present a smeared behavior in the brominated crystals and one of them seems to be related to the freezing of polar domains (T_f) while the other one was interpreted as a freezing of the soliton lattice (T_S). The thermal hysteresis effects are strongly enhanced with the increase of Br^- content.[11]

In a work on brominated BCCD by Ao *et al.*,[15] Raman spectra of 6.4% Br^--doped BCCD were found very similar to the spectra of the pure compound in the corresponding phases. In the region of external vibrations the number of lines was found to be identical, except for the strongly overlapped groups of lines where the generally increased linewidths in the doped sample jeopardize the resolution of such groups. Further comparative Raman and IR studies showed that at ambient pressure the low-temperature phases are modulated.[15–17] The temperature and pressure dependencies of the modulation in several Br^--doped crystals have been determined by means of IR spectroscopy.[18] Recently, Raman, IR, and dielectric studies of Br^--doped crystals were reported and the corresponding T-x phase diagram was presented.[11,19,20]

Although previous Raman and IR investigations[15–20] constitute serious pieces of experimental work, the vibrational modes associated with Cl^-/Br^- substitution were not identified. As follows from the structural data,[4] the H bonds and consequently interconnection between layers in the crystal structure of BCCD should be very sensitive to the Cl^-/Br^- substitution. To the best of our knowledge, this aspect was not studied so far. The microscopic mechanisms leading to the suppression of modulated C phases and the lack of the uniform ferroelectric phase in Br^--doped BCCD are not yet understood.

In this work we focus on the effects of Br^- impurities in BCCD through the study of the external modes and internal vibrations of water molecules by means of a Raman-

scattering technique. The respective experimental data obtained from 4%, 12%, and 24% brominated BCCD single crystals are compared with the spectra of nominally pure BCCD. Our results presented in this paper clearly show two principal consequences of the Cl^-/Br^- substitution in BCCD: (1) Due to the mass effect, Br^- ions induce some transformations in the low-frequency Raman spectra related to the external vibrations. As a result of a comparative analysis of experimental data, an interpretation of some low-frequency external mode behavior of the BCCD:Br system is given. (2) Incorporation induces partial weakening of the H bonds between layers in the crystal structure of BCCD. Detailed analysis of experimental results revealed some important features of hydrogen bonding in BCCD, and in particular, showed the influence of Br^- impurities on the phase-transition sequence in the BCCD:Br system. It is shown that hydrogen bonding is not involved in the mechanisms leading to the N-INC phase transition. Except for the shift of T_i, this transition is not seriously affected by bromination, whereas the phase-transition sequence at lower temperatures is deeply modified. The observed temperature dependence of the O—H stretching and external vibrations suggests the gradual formation of a heterophase state caused by Br^- pinning. Due to the weakening of hydrogen bonds in brominated samples the localization of protons is not accomplished down to 12 K. As a consequence, the nonmodulated FE phase is suppressed by bromination.

II. EXPERIMENTAL DETAILS

The single crystals of partially brominated BCCD were grown by slow controlled evaporation from the aqueous solutions of partially brominated calcium chloride and betaine. The bromine concentration in the samples used in this work was inferred from the studies reported by Le Maire[19] on the solid-state solubility of the system, and confirmed by the values of T_i and T_f determined experimentally by dielectric measurements for each sample used in Raman measurements. $T_i = 164$, 159, and 145 K for pure, 4%, and 12% brominated BCCD samples, respectively.

Polarized Raman spectra have been measured on samples in the form of carefully oriented and optically polished rectangular parallelepipeds $4\times3\times2$ mm^3 with the axes X, Y, and Z parallel to [100], [010], and [001], respectively. The crystallographic axes were determined with an accuracy of $\pm1°$ by x-ray diffraction.

Raman spectra were excited using the polarized light of an Ar^+ laser coherent INNOVA 90 ($\lambda = 514.5$ nm) in a right-scattering geometry. The scattered light was analyzed using a Jobin Yvon T64000 spectrometer equipped with a charge-coupled device and a photon counting detector. The spectral slit width was about 1.5 cm^{-1}.

The samples were placed in a closed-cycle helium cryostat with a temperature stability of about ±0.2 K. The actual sample temperatures were estimated to differ by less than 1 K from the temperature measured with a silicon diode attached to the sample holder. The temperature homogeneity in the sample was achieved with a copper mask setup.

III. RESULTS AND DISCUSSION

A. Influence of Br^- defects on the external vibrations in BCCD

1. Raman spectra in the normal phase

The isomorphic substitution of Cl^- by Br^- causes remarkable transformation of the low-frequency Raman spectra related to the external vibrations. The low-frequency modes assignment in BCCD is of particular interest, since in 1990 Dvořák[21] suggested that large amplitude librations of the betaines and of the inorganic ''Ca'' octahedra could be associated with the lowest-frequency Raman- and IR-active modes. These librations were considered as critical degrees of freedom in the phase-transition sequence of BCCD.

The symmetry of external modes can be obtained from standard factor-group analysis. In the normal phase of BCCD this analysis yields

$$\Gamma_{ext} = 14A_g + 13B_{1g} + 14B_{2g} + 13B_{3g} + 13A_u + 13B_{1u} + 12B_{2u} + 13B_{3u}. \quad (1)$$

Raman-active external vibrations of the Cl^- ions, localized in general positions, are

$$\Gamma_{ext}(Cl^-) = 3A_g + 3B_{1g} + 3B_{2g} + 3B_{3g}. \quad (2)$$

As the atomic mass of the Br^- is nearly twice that for Cl^-, detectable frequency shifts of the corresponding translational modes, in partially brominated samples, are expected. To obtain relevant information it is important to consider all external vibrations and their Cl^-/Br^- substitution dependence. Figure 2 shows that the low-frequency Raman spectra exhibit a gradual transformation when Br^- concentration increases. In general, the intensity of the Raman peaks decreases considerably by bromination, revealing in this way, strong alteration of the values of the polarizability tensor components. The number of Raman lines is practically the same for all the samples studied, and only one additional peak localized at 80 cm^{-1} was detected in $A_g(zz)$ geometry in the 24% brominated sample.

The low-frequency spectra for all scattering geometries were fitted with a sum of independent damped harmonic oscillators (IDHO) and their detailed comparison is given in Table II, for pure and 24% Br^--doped BCCD. An important finding is that frequencies of the lowest-lying modes at 33 cm^{-1} (A_g), 26 cm^{-1} (B_{1g}), and 22 cm^{-1} (B_{3g}) are independent of Br^- concentration, as can be seen in Fig. 2. Therefore, they can be unambiguously assigned to the external vibrations of betaine molecules. The lattice phonons sensitive to Cl^-/Br^- substitution are found at higher frequencies (above 44 cm^{-1}). These results support Dvořák's assumption about librations of betaines. Far-infrared measurements in brominated crystals are obviously required to complete the mode assignment.

Figure 3 presents the bromine content dependence of the low-frequency modes in $B_{1g}(xy)$ geometry, where there are more than three peaks sensitive to bromination. For other species, we found a similar result, which clearly shows that the substitution of Cl^- by Br^- ions affects not only the

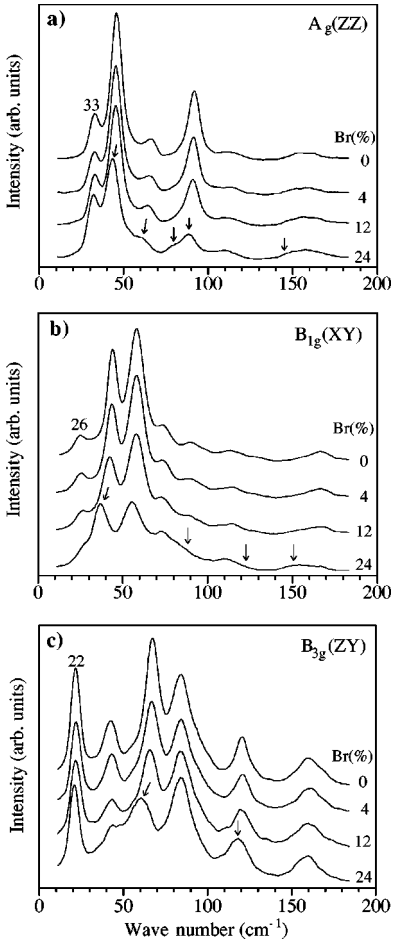

FIG. 2. Room-temperature Raman spectra of nominally pure and brominated BCCD in the region of external vibrations for selected scattering geometries. The arrows mark modes that are sensitive to bromination.

proper Cl^- translations, but also the force constants for surrounding environments, namely, water molecules, which inevitably influences the peculiarities of the modulation of the BCCD:Br system.

To see to what extent the hydrogen bonds are influenced by bromination, it is important to identify water translations and librations in pure and Br^--doped samples. From a comparative analysis of the low-frequency Raman spectra of pure BCCD and its partially deuterated analog, DBCCD (only the protons in the water molecules and partially in the CH_2 and CH_3 groups are replaced by deuterons), we can assign translations and librations of the water molecules.[22] The water libration band has been observed in the *xx* geometry (see Fig. 4) at 570 cm^{-1}. This band exhibits a typical broad line shape and a perfect shift in the deuterated sample with the ratio $\omega_H/\omega_D=1.36$. The corresponding band in the 24% brominated sample as well as the ones at 92 cm^{-1} and at 102 cm^{-1} are broadened and smeared, showing that random bromination induces disorder in the crystal lattice.

Weak and broad peaks in the range 150–170 cm^{-1} are attributed to water translations. As can be seen in Fig. 4, the peak at 164 cm^{-1} in the pure BCCD exhibits a shift down to 156 cm^{-1} in the partially deuterated sample. The corresponding ratio $\omega_H/\omega_D=1.05$ is in quite good agreement with the isotopic shift of water translations in solid hydrates.[23] It is interesting to remark that in the 24% brominated sample, the above-mentioned peak exhibits a slight but a trusty downward shift. Similar effects can be seen in the frequencies of the other A_g and B_{1g} modes listed in Table II. In B_{3g} spectra there is not a noticeable shift, but there is a transformation of the line shape of strongly overlapped peaks in the same frequency interval. These facts indicate some changes in the hydrogen bonding, obviously correlated with the increase of the Br^- concentration.

TABLE II. Frequencies (in cm^{-1}) of Raman peaks observed in nominally pure and 24% brominated BCCD at room temperature w stands for very weak peaks which are hardly seen after reduction; a star stands for modes shifted in the brominated sample.

$A_g(zz)$		$B_{1g}(xy)$		$B_{2g}(xz)$		$B_{3g}(yz)$	
0%	24%	0%	24%	0%	24%	0%	24%
						22	22
		26	27				
33	32						
46	43*	44	37*	46	38*	44	45
		59	57	56	54	56w	55w
67	60*					67	62*
		75	74	74	73		
	80*					85	85
93	89*	92	86*			95w	96w
				100	92*		
114	111	115	112	112	111		
						121	118*
		134w	127w*	136	128*		
152	146*						
		158w	150w*				
162	160					160	159
		167	165	168	167	169	168
		194	194				
208	204						
				220	220		
230	230						

2. Temperature dependence of external vibrations

As it was reported by Ao and Schaack in their pioneering paper,[24] the low-frequency Raman spectra of pure BCCD are drastically affected by the phase transitions. The most interesting is the *xz* scattering geometry where transitions between the principal phases can be clearly seen in the spectral range below 40 cm^{-1}. The temperature dependence of the low-frequency *xz* Raman spectra of pure, 4%, and 12% brominated BCCD is presented in Fig. 5. All these spectra were recorded under similar experimental conditions.

At room temperature, the lowest-lying Raman band in the *xz* geometry, which corresponds to B_{2g} phonons in the N phase, was observed at 46 cm^{-1}. In brominated samples this peak is shifted down to 38 cm^{-1} and can be seen down to 12 K in Figs. 5(b) and 5(c). In the INC phase B_{2g} modes from

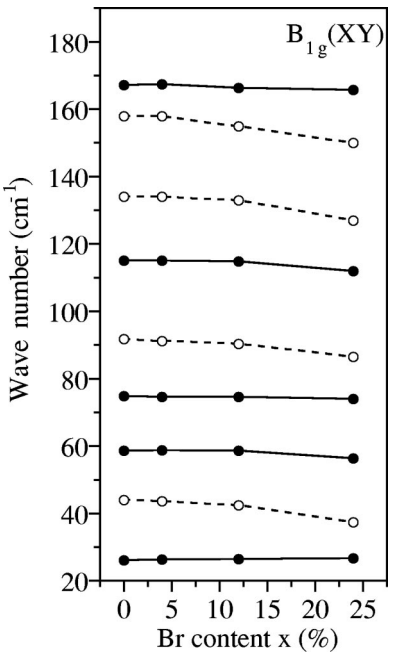

FIG. 3. Frequency of the fitted Raman peaks as a function of the bromine content.

the interior of the Brillouin zone start to appear. IR-active B_{1u} zone-center modes of the parent N phase become Raman active at the lock-in phase transition due to the point-group symmetry lowering: $Pnma \rightarrow P2_1ca$.

Detailed interpretation of the low-frequency *xz* Raman spectra of pure BCCD in the INC and 1/4 phases was recently reported by Hlinka *et al.*[25] Briefly, the peak at 25 cm^{-1} (value at 80 K) was assigned to a B_{2g} folded phonon. As there are no other peaks below 30 cm^{-1} in the N phase, both in *xz* (B_{2g}) and in *z* (B_{1u}) spectra, the two low-frequency *xz* modes at 12 and 19 cm^{-1} were interpreted as arising in the modulated 1/4 phase due to the folding of the B_{1u} branches at $\mathbf{q}=\mathbf{c}^*/4$. One of them is an optic mode carrying almost all damping and strength, and another one

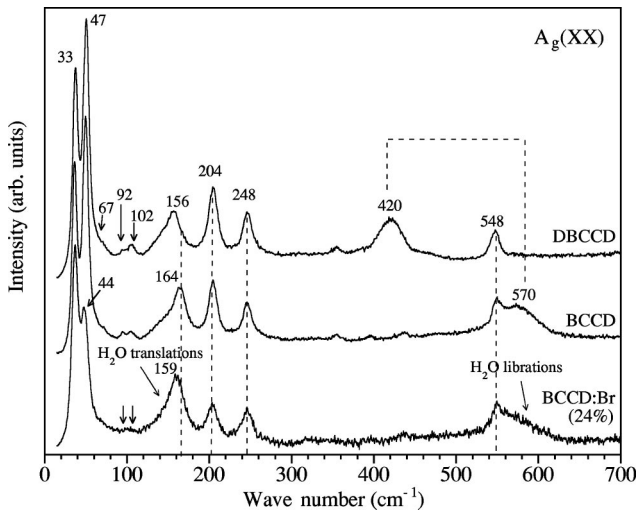

FIG. 4. Low-frequency *xx* Raman spectra of nominally pure, deuterated, and 24% brominated BCCD (labeled on the curves) at room temperature. Vertical dashed lines are guides for the eyes.

with a small damping is originated from the transverse-acoustic (TA) mode. These two modes are coupled and a coupled damped harmonic-oscillators (CDHO) model was successfully applied to evaluate the temperature dependence of their parameters.[25] That optical mode was identified as the pseudophason.[25]

At the transition to the nonpolar 1/5 phase, changes in the Raman selection rules occur. The *xz* spectra possess B_2 symmetry and the B_{2g} folded mode from the N phase is still active, but modes activated from B_{1u} branches in the 1/4 phase are now extinct and B_{2u} modes of the parent phase should appear in the 1/5 phase. Accordingly, the B_{2g} mode at 28 cm^{-1} still exists in the temperature range of the 1/5 phase, the two coupled low-frequency peaks disappear abruptly, and new peaks at 17 and 26 cm^{-1} arise. The former peak is an activated TA mode and the sharp peak at 26 cm^{-1} is originated from the B_{2u} mode observed in IR spectra.[26,27] The next principal 1/6 phase is polar along *x* as well as the

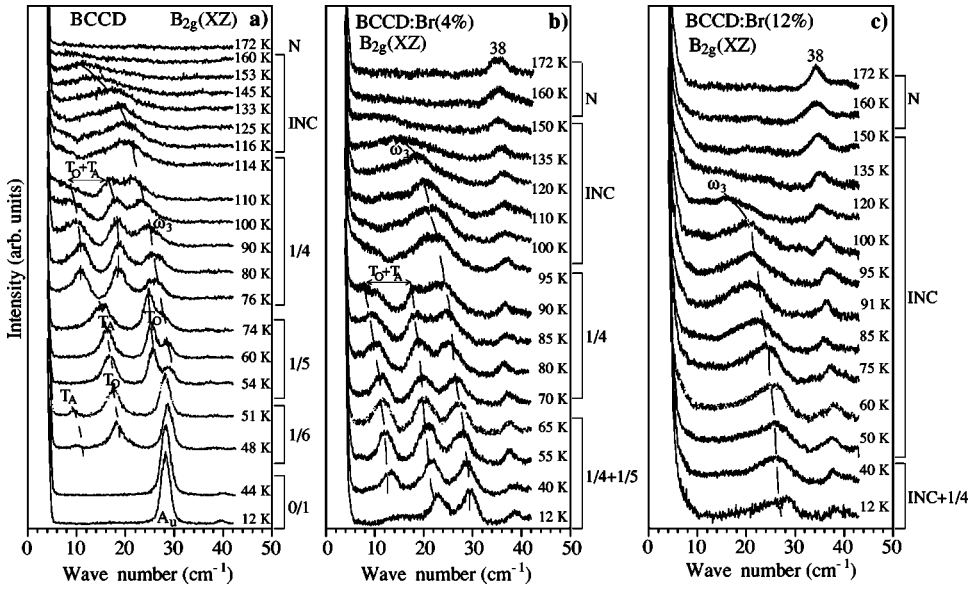

FIG. 5. Temperature dependence of Raman spectra of (a) nominally pure, (b) 4% brominated, and (c) 12% brominated BCCD in the low-frequency region in *xz* scattering geometry. Principal phases of the brominated system are indicated.

1/4 phase and therefore the corresponding selection rules are recovered. The B_{1u} modes are now active instead of B_{2u} ones, but both TA and optic modes activated in the 1/6 phase are now well separated and have lower frequencies with respect to the 1/4 phase, since phonons with wave vectors closer to the zone center are now activated. Coupling between them does not occur and an IDHO model can be used to fit the experimental spectra.

Finally, in the nonmodulated FE phase (below 46 K) all folded acoustic and optic modes disappear and only A_u modes, silent in the parent N phase, acquire A_2 symmetry and become active in xz Raman spectra. This mode has been observed in IR spectra[27] and neutron-scattering experiments.[28]

In the brominated crystals, T_i is shifted to lower temperatures and B_{2g} modes from the interior of the Brillouin zone start to appear below 159 and 145 K in 4% and 12% brominated samples, respectively. Transformations of the Raman spectra at the lock-in phase transition are rather smooth. As can be seen in Fig. 5(b) the low-frequency xz Raman spectra of the 4% brominated crystal below 100 K are quite similar to those of the pure BCCD in the 1/4 phase. Moreover, these spectra have a characteristic antiresonance line shape with the deep minimum near the pure TA frequency ($\sim$16 cm^{-1}). Due to the random substitution of Cl^- by Br^-, the translational symmetry is partially broken and all Raman peaks are considerably broadened. The sharp minimum at $\sim$16 cm^{-1} observed in the pure BCCD due to the phonon modes coupling is also smeared in the 4% brominated sample. The CDHO model used in Ref. 25 was successfully applied to fit experimental spectra of the 4% brominated crystal below 100 K. The low-frequency Raman spectra were first fitted with a sum of three IDHO and a strong discrepancy between experimental data and fitting results was found. A good fit was achieved when the two lowest peaks were coupled by way of a CDHO formula[25] and the third mode (ω_3) was considered as independent. Both fitting results are compared in Fig. 6. The values of the frequencies ω_+, ω_-, and ω_3 (the IDHO model) as well as ω_0 and ω_A (the CDHO model) were found quite close to those in the pure BCCD, but the value of the bare acoustic mode damping γ_A is remarkably larger (1.6 cm^{-1} instead of 0.2 cm^{-1}). In pure BCCD the frequency and damping (γ_{AP} in Fig. 6) of the activated TA mode are virtually temperature independent in the whole temperature range of the 1/4 phase, 115–75 K.[25] In the 4% brominated sample γ_A is also temperature independent in the range 100–60 K, but it increases as the temperature decreases below 60 K. This temperature was quoted in the T-x diagram[19,20] as T_f, which marks the transition to the frozen state.

On further cooling, xz Raman spectra of the 4% brominated sample exhibit a rather smooth temperature dependence, and a weak hardening can be traced down to 12 K. There is no clear indication of the phases transition to the next modulated phase. Neither the 1/5 nor the 1/6 C phases are established in the long-range scale. In fact, for brominated samples all the peaks in the low-frequency region remain broad down to 12 K, which is a manifestation of a violation of the long-range order. In recent neutron-scattering

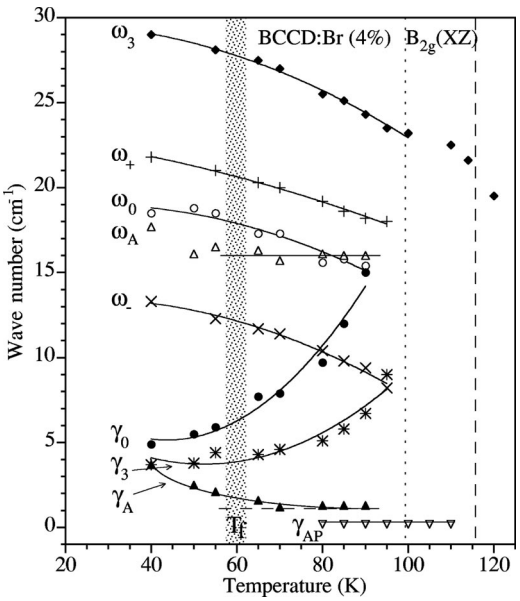

FIG. 6. Temperature dependence of the oscillator parameters (connected by eye-guiding solid lines) as obtained from the CDHO fits for the xz Raman spectra of the 4% brominated BCCD. ω_+ and ω_- correspond to the alternative fits with the IDHO model. Temperature dependence of the damping parameter of the activated acoustic mode γ_{AP} (down triangles) from the corresponding spectra of pure BCCD is given for comparison. Verticals dashed and dotted lines mark the lock-in phase-transition temperature in pure and 12% brominated BCCD, respectively. The stripe marks T_f in 12% brominated BCCD.

experiments,[14] the coexistence of several C phases, 1/4, 4/17, 2/9, and 1/5, has been revealed below 62 K in the 4% brominated (but partially deuterated) sample. The widths of the corresponding satellites are very large because of a small coherence length of the periodic modulation. Apparently, a heterophase state is responsible for the observed Raman peaks broadening. At lower temperatures (40–12 K) no coupling between optic and acoustic branches occurs in the 4% brominated sample. The rather broad feature at about 16 cm^{-1}, observed at 12 K [see Fig. 5(b)], reflects the density of states of acoustic branches of the frozen heterophase state.

In the 12% brominated crystal the N-INC phase transition occurs at 145 K and the B_{2g} folded mode starts to appear in the xz Raman spectra presented in Fig. 5(c). This peak is extremely broad down to 12 K and apparently reflects the density of states of the corresponding branch. There is no indication of the phase transition to the long-range 1/4 C phase in the whole temperature range studied.

B. Influence of Br^- on the hydrogen bonding in BCCD

A comparative analysis of the low-frequency Raman spectra in BCCD and in Br^--doped BCCD showed that Cl^-/Br^- substitution induces some changes in the hydrogen bonding. To obtain more detailed information about the influence of bromine on the hydrogen bonding, we have compared the O—H stretching bands at $\sim$3400 cm^{-1} in the pure and in the brominated samples. Polarized Raman spec-

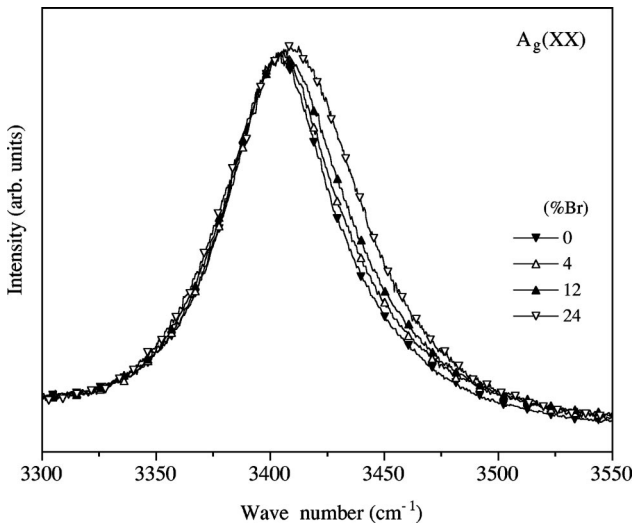

FIG. 7. Normalized Raman spectra of nominally pure and brominated BCCD in the region of the O—H stretching vibrations at room temperature.

tra, observed in the corresponding spectral region, are similar to those obtained in the pure BCCD.[22] However, some important features must be pointed out: both the linewidth and the frequency of the O—H stretching band increase with increasing bromination, as can be seen in Fig. 7. The upward frequency shift of this band is direct evidence of the weakening of the O—H bonding in brominated crystals, since Br^- has smaller proton acceptor strength than Cl^-[23]. Moreover, Br^- ions cause local distortions and partially break translational symmetry. The observed broadening is due to broader distribution of O—H bond lengths in brominated crystals. This is an important finding since O—H$\cdots$Cl (Br) bonds are linking the layers lying in the mirror *m* planes, which are $b/2$ apart in the N phase. The alteration of the interactions between these layers and violation of translational symmetry are responsible for the deep transformations introduced by bromination, in the modulated phases of BCCD. A comparative analysis of the temperature dependence of the O—H stretching vibrations is presented in the next sections.

1. Order parameter behavior in the incommensurate phase

As hydrogen bonds link neighboring layers, their stretching vibrations must be very sensitive to the corrugation of these layers in the modulated phases. In this section we shall consider the influence of the Br^- impurities on the hydrogen bonding in the INC phase.

In the brominated crystals, T_i is shifted down to 159 K and 145 K in the 4% and 12% brominated samples, respectively. The 2/7 C phase quoted at about 110 K for 4% brominated BCCD (Refs. 19 and 20) was not detected in our experiments. In the INC phase, Raman spectra of brominated crystals in the region of the O—H stretching vibrations exhibit a temperature dependence quite close to pure BCCD.

The temperature dependence of the frequencies of the fitted Raman peaks in $A_g(xx)$ geometry for pure and 12% Br^--doped BCCD is shown in Fig. 8. The two main peaks (marked by the arrows in the lower inset in Fig. 8) exhibit different temperature dependencies ($d\nu/dT<0$ for the higher-frequency component and $d\nu/dT>0$ for the lower frequency one). This behavior of the ν_1^ω mode is evidence of the modulated structure of pure and brominated BCCD. The existence of two branches in the high-temperature range of the INC phase is related to a sinusoidal regime and the splitting $\Delta\nu$ between the two band singularities[22,29] gives a measure of the order-parameter amplitude on an appropriate scale. Representing by β its critical exponent we can write $\Delta\nu=\alpha(T_i-T)^\beta$. The upper inset of Fig. 8 shows the fitted curves to the experimental data: we obtained $\alpha=12\pm1\,\mathrm{cm}^{-1}$ and $\beta=0.35\pm0.02$ cm^{-1} for BCCD and $\alpha=14\pm1\,\mathrm{cm}^{-1}$ and $\beta=0.32\pm0.02$ cm^{-1} for 12% Br^- doped BCCD.

Additional rather weak components between the two main peaks become visible below 140 K for BCCD and below 100 K for the brominated system. They must be associated with the onset of a nonsinusoidal regime in the INC phases.[22]

By comparing the experimental results obtained in both systems we can argue that in the INC phase the behavior of the order parameter amplitude is similar in both systems (except for the shift of T_i). So, we can conclude that the hydrogen bonding is not seriously involved in the mechanisms leading to the N-INC transition.

2. Hydrogen bonds in the C modulated phases and effect of bromination

Detailed Raman study of the O—H stretching vibrations in pure BCCD down to 12 K has revealed interesting features clearly related to the wealth of its structural phase transitions.[22] In fact, Raman spectra reflect a sequential distortion of water molecules. In this connection, we performed a comparative analysis of the O—H stretching vibrations in a broad temperature range, to elucidate the influence of the Br^- impurities of the hydrogen bonding and local distortion of the water molecules at phase transitions (if any) between principal C phases.

Due to changes in Raman selection rules at each transition between the principal C phases, one can expect transformations in the region of the O—H stretching vibrations. The factor group analysis for the internal vibrations of the water molecules in BCCD predicts single ν_1^ω and single ν_3^ω bands for each scattering geometry in the N phase.[22] The asymmetrical ν_3^ω stretching mode is rather weak in Raman spectra and can be clearly seen only at low temperatures. In all principal C phases, with C_{2v} or D_2 point group symmetry, all phonons become simultaneously IR and Raman active and additional components may appear due to Brillouin zone folding. However they may be strongly overlapped and poorly resolved if the corresponding phonon branch is flat. In the nonmodulated ($\delta=0$) FE phase (point group C_{2v}) one can expect two ν_1^ω and two ν_3^ω bands for each species since there are two kinds of water molecules localized in the fourfold C_1 sites.

The changes of symmetry between the principal C phases of BCCD are well reflected in the (yz) component of the Raman tensor. The corresponding changes of selection rules are the following:

$$B_{3g}(N)\rightarrow A_2(1/4)\rightarrow B_3(1/5)\rightarrow A_2(1/6)\rightarrow B_1(0/1). \quad (3)$$

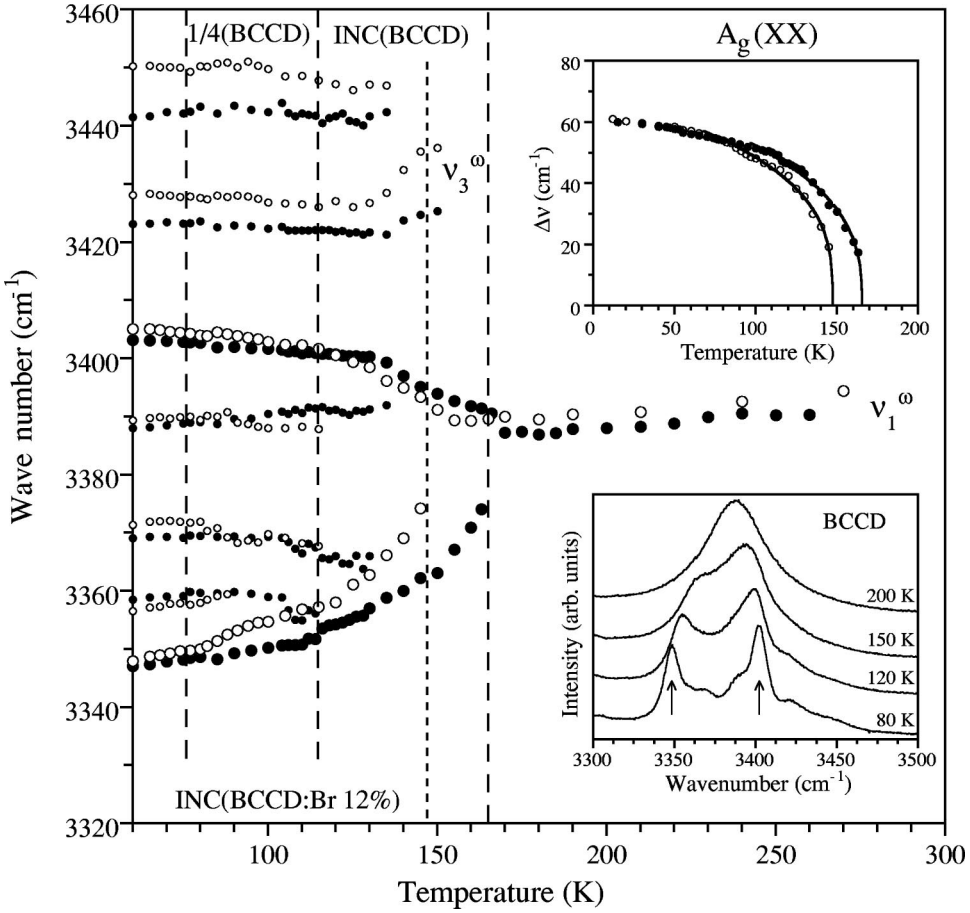

FIG. 8. Temperature dependence of the frequencies of the fitted Raman peaks for nominally pure (full symbols) and 12% brominated (open symbols) BCCD in $A_g(xx)$ geometry. Vertical dashed lines mark the phase-transition temperatures in pure BCCD, and the dotted line marks T_i in 12% brominated BCCD. The lower inset shows the temperature dependence of Raman spectra of pure BCCD in the region of the O—H stretching vibrations in $A_g(xx)$ geometry. The upper inset shows the temperature dependence of the splitting between the two main peaks indicated by arrows in the lower inset and larger symbols in this figure.

Accordingly, for each principal phase of the pure BCCD, we have obtained peculiar Raman spectra of the O—H stretching vibrations in the *yz* geometry, which are presented in Fig. 9. The sequential distortion of water molecules at the phase transitions can be traced clearly. At the transition to the nonmodulated FE phase, at 46 K, all the folded modes disappear and the spectra become simpler.

As shown in Fig. 9, just below T_i, Raman spectra of pure and brominated crystals are similar. As in pure crystals, the O—H stretching band at $\sim$3400 cm^{-1} in the brominated crystals exhibits a splitting into several components and on further cooling, the separation between them increases. The frequency difference of these components is a measure of the water molecules' distortion, which is caused by the different intermolecular bonding via H bonds with the nearest Cl^- (Br^-) ions. From the observed Raman patterns one can as-

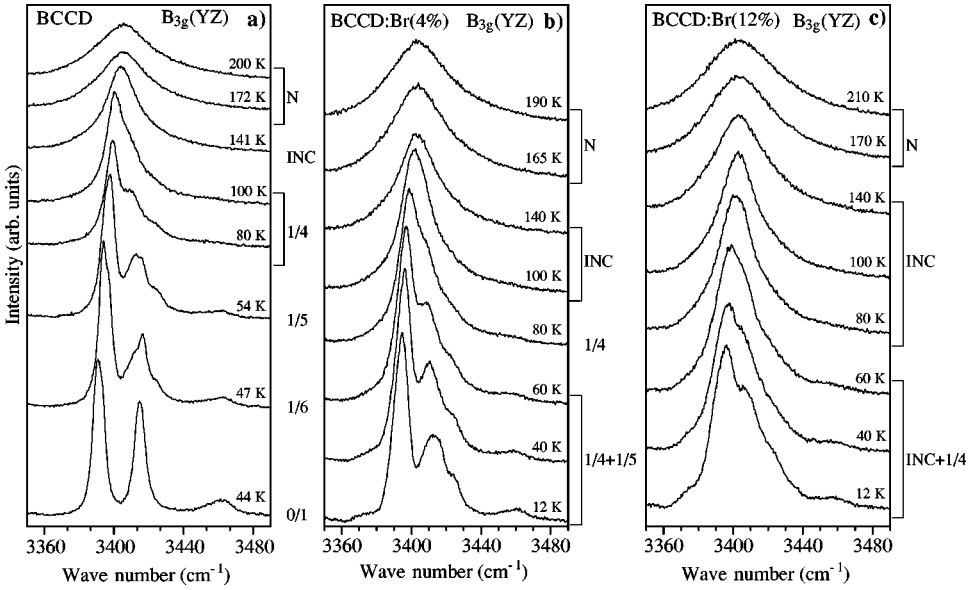

FIG. 9. Temperature dependence of Raman spectra of (a) nominally pure, (b) 4% brominated, and (c) 12% brominated BCCD in the region of stretching vibrations of the water molecules in *yz* scattering geometry. Principal phases of the brominated system are indicated.

sume that local distortion of the water molecules in the 4% brominated sample corresponds to the 1/4 phase in between ~100 K and 60 K. Raman spectra, in the spectral range 3200-3600 cm^{-1}, taken below 60 K in the 4% Br^--doped sample, can be well fitted with a weighted sum of the spectra of pure BCCD in 1/4 and 1/5 phases. Very likely, below 60 K, the coexistence of 1/4 and 1/5 modulations occurs due to an inhomogeneous distribution of defects in this sample.

The temperature dependence of the O—H stretching vibrations in the 12% brominated sample in the *yz* geometry is rather smooth (the fitting results are hardly unique) and the observed line shape corresponds to an INC phase in the whole temperature interval below ~140 K. Down to 12 K all the bands in this sample are broadened with respect to their analogs in pure BCCD. Folded modes can be seen down to 12 K, and the observed Raman pattern suggests the presence of domains of the 1/4 C phase below ~60 K. In case of homogeneous distribution of defects, $x=12$ is equivalent to about one Br^- ion per unit cell of the N phase. Apparently Br^- impurities not only break translational symmetry, but also induce weakening of the interlayer hydrogen bonds and prevent in this way long modulated regular corrugation of the layers along four, five or more unit cells. As a consequence INC modulation persists down to the lowest temperature. In case of inhomogeneous Cl^-/Br^- substitution one can expect formation of rather small C modulated domains in the corresponding poor brominated regions of the sample.

These results show that the low-temperature ''frozen state'' in brominated crystals[11,19,20] is a heterophase state where several C phases coexist. It is important to outline that any fingerprints of the nonmodulated FE phase were not observed in the brominated samples, down to the lowest temperature studied. Lack of the nonmodulated FE phase in the brominated crystals is discussed in the next section.

3. Nonlocalization of protons in O—H bands in brominated crystals

The temperature dependence of the O—H stretching band in the 12% brominated BCCD in *zz* geometry is presented in Fig. 10, where the spectra of pure BCCD recorded at 200 and 12 K are also presented for comparison. Due to the strong asymmetry of the O—H···Cl bonds in pure BCCD, the O—H stretching vibrations are localized in the uniform FE phase and form well-separated sharp peaks at 3387 cm^{-1} and 3413 cm^{-1}, followed by a weak peak at 3450 cm^{-1}.[22] The O—H stretching band at ~3400 cm^{-1} in the 12% brominated crystal exhibits a splitting below T_i and on further cooling additional components start to appear. Applying the fitting procedure over the entire temperature interval, we have found a temperature dependence of their frequencies, which is presented in Fig. 11. As can be seen in Figs. 10 and 11, in the 12% brominated crystal, the splitting between the two main components is much smaller than in the corresponding spectrum of pure BCCD. Moreover, there are two weak bands activated due to Brillouin-zone folding, which persist down to 12 K. Similar effects have been also observed in the 4% brominated sample. This behavior suggests that hydrogen bonds between neighboring layers in brominated crystals exhibit smaller distortions, and the localization of protons, typical for the nonmodulated FE phase, is not accomplished down to 12 K.

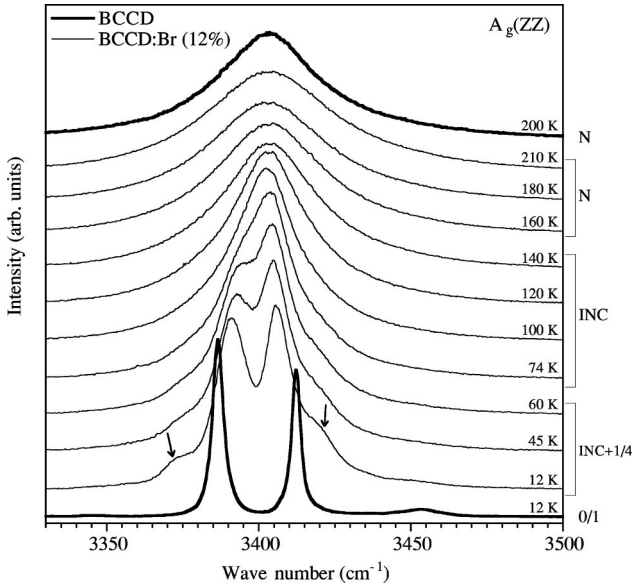

FIG. 10. Temperature dependence of Raman spectra of the 12% brominated BCCD in the region of stretching vibrations of the water molecules in *zz* scattering geometry. Raman spectra of nominally pure BCCD (bold curves) in the N and FE phases at 200 and 12 K, respectively, are shown for comparison. The arrows mark the $\mathbf{q}\neq 0$ folded modes observed in 12% brominated crystals down to 12 K.

We assume that in brominated crystals the nonmodulated FE phase is missing due to peculiar positions of impurities. Namely, as was mentioned in the Introduction, the Br^- ionic radius is larger than that of Cl^- and partial bromination increases the average size of the unit cell in the N phase.[15] Note that this enlargement occurs mostly along the *b* direc-

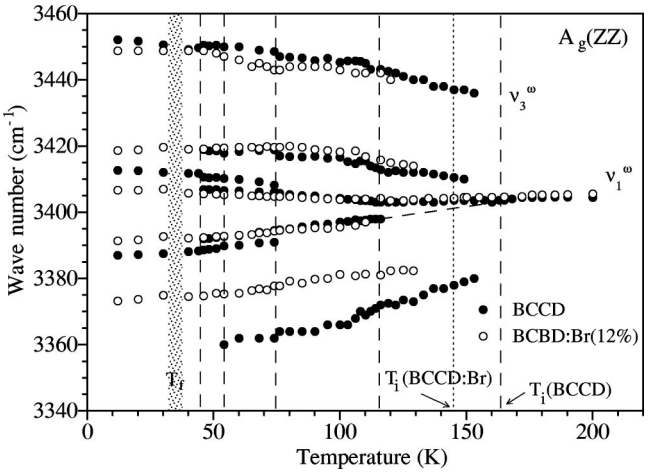

FIG. 11. Temperature dependence of the frequencies of the fitted Raman peaks shown in Fig. 10 for nominally pure (full symbols) and 12% brominated (open symbols) BCCD. Vertical dashed lines mark the phase-transition temperatures in pure BCCD, and the dotted line and stripe mark T_i and T_f, respectively, in 12% brominated BCCD.

tion. Since Cl^- occupies interlayer sites in the unit cell (see Fig. 1), partial substitution of Cl^- by Br^- increases the average distance between layers connected via O—H$\cdots$Cl (Br) bonds. As a consequence, partial weakening of the O—H bonding around Br^- ions is obviously expected. Our Raman measurements confirm the expected weakening. Due to thermal contraction, the layers naturally press on together on cooling, and in pure BCCD, the phase transition to the nonmodulated FE phase, accompanied with the localization of protons, occurs at 46 K. Owing to Br^- incorporation, the neighboring layers are not so close to each other and a similar localization in brominated crystals cannot occur. Consequently, the FE state cannot be properly established. Local distortions associated with Br^- impurities partially break the translational symmetry and lead to the activation of $\mathbf{q}\neq 0$ phonons observed in brominated crystals down to 12 K (see Fig. 10). This interpretation correlates well with previous high-pressure measurements. The onset of the nonmodulated FE phase occurs in brominated crystals ($x<8\%$) on cooling, at sufficiently high pressure.[17,19] This pressure reduces interlayer distance and ''compensates'' for the weakening of the hydrogen bonding induced by bromination.

IV. CONCLUSIONS

The analysis of the low-frequency Raman spectra of pure and partially brominated crystals showed that the lowest-frequency Raman-active phonons are associated with the betaines vibrations, whereas the lattice phonons sensitive to Cl^-/Br^- substitution are found at higher frequencies (above 44 cm^{-1}). Both translational and internal vibrations of the water molecules in BCCD are affected by the partial substitution of Cl^- by Br^- ions, due to peculiar positions of these entities in the unit cell.

The O—H stretching mode evidences the modulated structure of pure and brominated BCCD, and the order-parameter amplitude is proportional to the splitting of the ν_1^{ω} mode below T_i. The critical exponents related to the primary order parameter are equal in the pure and 12% Br^--doped BCCD within the experimental error. This result suggests that hydrogen bonds are not seriously involved in the mechanism of the N-INC phase transition governed by the low-frequency Λ_3 soft mode. In contrast, weakening of the hydrogen bonding in brominated crystals plays an important role at the further phase-transition sequence at lower temperatures, and deeply modifies the devil's staircase behavior.

Analysis of the temperature dependence of the O—H stretching and external vibrations of the 4% brominated crystal allows us to conclude that only the 1/4 C phase exists in this crystal in the long-range sense. Due to the random substitution of Cl^- by Br^-, the translational symmetry is partially broken and all Raman peaks are considerably broadened. A remarkably broadened pseudophason gap has been observed below 100 K in this crystal. Its further broadening below $T_f\sim 60$ K, as well as the rather gradual temperature evolution of external and the stretching O—H modes, suggests that the low-temperature frozen phase is a heterophase state caused by impurity pinning. The study of the internal modes of the water molecules confirmed that short-range distortions, typical of 1/4 and of 1/5 modulations, occur in the 4% brominated sample. The low-frequency spectra show that neither the 1/4 phase nor the 1/5 phase exists alone below T_f.

In the 12% brominated crystal, the averaged distance between impurities is comparable with the unit-cell parameter of the N phase. For such a high concentration of pinning centers the long-range order of the soliton lattice is destroyed. Inhomogeneity of Br^-/Cl^- substitution is more likely to occur, and the soliton lattice acquires a rather irregular structure: a randomly distributed coexistence of solitons. On cooling, one can expect a rather diffusive temperature evolution into a frozen state of irregular discommensurations. The Raman spectra presented in Fig. 5(c) confirm this scenario. C phases with long modulation wavelengths are completely suppressed in the 12% Br^--doped crystal.

Finally, the Br^- impurities mostly affect the low-temperature phase transition into the homogeneous FE phase. As was shown in our recent paper,[22] the FE transition, at 46 K, in the pure BCCD, is associated with the localization of protons in the strongly asymmetrical O–H$\cdots$Cl bonds. For a high enough concentration of Br^-, the nonmodulated FE phase is missing and modulated phases are observed down to the lowest temperature investigated (12 K). These results allow us to conclude that the localization of protons is not accomplished down to 12 K, in both brominated samples studied, because Br^- ions weaken the H bonds.

ACKNOWLEDGMENTS

We thank gratefully Dr. J. Albers for his collaboration in the study of betaine compounds. The authors thank A. Costa for his technical assistance. This work was supported by the projects PRAXIS XXI/3/3.1/MMA/1769/95 and PRAXIS XXI/P/FIS/14287/1998. Yu. I. Yuzyuk and Filipa Pinto thank Projecto Praxis XXI for their grants: BCC/4463/96 and BICJ/4688/96, respectively.

*On leave from the Faculty of Physics, Rostov State University, Rostov-on-Don, Russia.

[1] J. Albers, A. Klöpperpieper, H. E. Müser, and H. J. Rother, Ferroelectrics **54**, 45 (1984).

[2] H. J. Rother, J. Albers, and A. Klöpperpieper, Ferroelectrics **54**, 107 (1984).

[3] W. Brill and K. H. Ehses, Jpn. J. Appl. Phys., Part 1 **24-2**, 826 (1985).

[4] W. Brill, W. Schildkamp, and J. Spilker, Z. Kristallogr. **172**, 281 (1985).

[5] J. M. Pérez-Mato, Solid State Commun. **67**, 1145 (1988).

[6] J. L. Ribeiro, M. R. Chaves, A. Almeida, J. Albers, A. Klöpperpieper, and H. E. Müser, J. Phys.: Condens. Matter **1**, 8011 (1989).

[7] H.-G. Unruh, F. Hero, and V. Dvořák, Solid State Commun. **70**, 403 (1989).

[8] J. L. Ribeiro, M. R. Chaves, A. Almeida, J. Albers, A. Klöpperpieper, and H. E. Müser, Phys. Rev. B **39**, 12 320 (1989).
[9] M. R. Chaves and A. Almeida, in *Geometry and Thermodynamics: Common Problems of Quasi-Crystals, Liquid Crystals and Incommensurate Insulators*, Vol. 229 of *NATO Advanced Studies Institute, Series B: Physics*, edited by J. C. Tolédano (Plenum, New York, 1991), p. 353.
[10] J. M. Ezpeleta, F. J. Zúñiga, W. Paulus, A. Cousson, J. Hlinka, and M. Quilichini, Acta Crystallogr., Sect. B: Struct. Sci. **52**, 810 (1996).
[11] G. Schaack and M. Le Maire, Ferroelectrics **208-209**, 1 (1998).
[12] J. M. Kiat, G. Calvarin, M. R. Chaves, A. Almeida, A. Klöpperpieper, and J. Albers, Phys. Rev. B **52**, 798 (1995).
[13] L. G. Vieira, A. Almeida, J. L. Ribeiro, M. R. Chaves, A. Klöpperpieper and J. Albers, Phys. Status Solidi B **204**, 863 (1997).
[14] L. G. Vieira, O. Hernandez, A. Almeida, M. Quilichini, J. L. Ribeiro, M. R. Chaves, and A. Klöpperpieper, Eur. Phys. J. B **10**, 447 (1999).
[15] R. Ao, G. Lingg, G. Schaack, and M. Zöller, Ferroelectrics **105**, 391 (1990).
[16] M. Le Maire, G. Lingg, G. Schaack, M. Schmitt-Lewen, G. Strauss, and A. Klöpperpieper, Ferroelectrics **125**, 87 (1992).
[17] M. Le Maire, A. López Ayala, G. Schaack, A. Klöpperpieper, and H. Metz, Ferroelectrics **155**, 335 (1994).
[18] M. Le Maire, A. Lengel, G. Schaack, and A Klöpperpieper, Ferroelectrics **185**, 217 (1996).
[19] M. Le Maire, Ph.D. thesis, Universität Würzbutg, 1996.
[20] M. Le Maire, R. Straub, and G. Schaack, Phys. Rev. B **56**, 134 (1997).
[21] V. Dvořák, Ferroelectrics **104**, 135 (1990).
[22] Yu. I. Yuzyuk, A. Almeida, M. R. Chaves, Filipa Pinto, M. L. Santos, L. M. Rabkin, and A. Klöpperpieper, Phys. Rev. B **62**, 14 712 (2000).
[23] H. D. Lutz, Struct. Bonding (Berlin) **69**, 99 (1988).
[24] R. Ao and G. Schaack, Indian J. Pure Appl. Phys. **26**, 124 (1988).
[25] J. Hlinka, I. Gregora, and V. Vorlíček, Phys. Rev. B **56**, 13 855 (1997).
[26] R. Ao and G. Schaack, Ferroelectrics **80**, 105 (1988).
[27] S. Kamba, V. Dvořák, J. Petzelt, Yu. G. Goncharov, A. A. Volkov, and G. V. Kozlov, J. Phys.: Condens. Matter **5**, 4401 (1993).
[28] R. Currat, J. F. Legrand, S. Kamba, J. Petzelt, V. Dvořák and J. Albers, Solid State Commun. **75**, 345 (1990).
[29] H. Poulet and R. M. Pick, in *J. Birman's Festchrift*, edited by M. Balkanski, M. Lax and H. R. Trebin (World Scientific, Singapore, 1993).